Multi-Mode Real-Time Strain Monitoring in Composites using Low Vacuum Carbon Fibers as a Strain Sensor under Different Loading Conditions

Yumna Qureshi*[(a)], Mostapha Tarfaoui*[(a)], Khalid Lafdi[(b,c)]

(a) ENSTA Bretagne, IRDL - UMR CNRS 6027, F-29200 Brest, France.

(b) University of Dayton, Nanomaterials Laboratory, Dayton, OH 45469-0168, United States

(c) Department of Mechanical and Construction Engineering, Northumbria University, Newcastle upon Tyne, UK

Abstract: Structural health monitoring is a vastly growing field consisting of sensors embedded in or attached with the structure which respond to the strain or other stimuli to monitor the deformation in real-time. In this study, a multi-mode strain detection is carried out in composites using nanomaterial-based sensor technology. A Carbon fiber (CF) sensor was developed using unidirectional carbon filaments aligned straightly together and its sensitivity was calculated experimentally, with gauge factor (GF) in 10.2-10.8 range. Then, this CF sensor is embedded gradually at different directions i.e. 0°,+45°,90°,-45° between the plies of composite for real-time/in-situ strain monitoring. The composite specimen was then cut in star profile, each leg demonstrating the direction of the CF sensors. These composite samples are then tested under tensile and flexural cyclic loading. There is a good reproducibility in the results and the mechanical response of composite correlated perfectly with the electrical resistance of the CF sensor. It can also be noted that the sensors, depending on their respective position, manage to faithfully reproduce the mechanical behavior of the specimen tested (traction/compression). The results established that the CF exhibited good

*Corresponding author:
E-mail address: yumna.qureshi@ensta-bretagne.org, mostapha.tarfaoui@ensta-bretagne.fr
Fax: +33 2 98 34 87 30

potential as flexible reinforcement for in-situ monitoring of composites and can provide detection over large sections and unapproachable locations. This study also showed that direction and position of the sensor plays a vital role in the detection, identification (whether its tensile or compressive) and quantification of the deformation experienced by the structure under different loading conditions.

Keywords: Composites, strain deformation, real-time monitoring system, carbon fiber sensor, multi-mode detection

Table of notation

T	*Test*
R	*Resistance*
GF	*Gauge Factor*
S	*Stress*
ST	*Strain*
A	*0°*
B	*45°*
C	*90°*
D	*-45°*
SA	*Sensor in position A*
SB	*Sensor in position B*
SC	*Sensor in position C*
SD	*Sensor in position D*

*Corresponding author:
E-mail address: yumna.qureshi@ensta-bretagne.org, mostapha.tarfaoui@ensta-bretagne.fr
Fax: +33 2 98 34 87 30

1. Introduction

Application of structural composites in the field of infrastructure, energy, aerospace, and automobile has been increasing rapidly and these structures often experience a variety of conditions such as impact, bending, elongation, shock loading, or environmental effects [1]ï [4]. The detection of local damage such as delamination, interlaminar failure, matrix softening, and matrix cracking in composites is often difficult to detect unless the performance of the materials has been compromised [5]ï [7]. Non-destructive techniques (NDT) such as ultrasonic detection, X-rays etc. can detect local damage however they often require disassembly of the structure for inspection and they arenôt able to detect damage in instantaneously. Acoustic emission is often used for real-time monitoring of the failure in structures but, interpretation of the data is a complex process and mostly qualitative. So, it is important to develop novel techniques to monitor the deformation of the structure in real-time, and structural health monitoring (SHM) is a renowned and extensively used system to study the behavior of the structure in real-time to guarantee their reliability and safety [8]ï [12].

Currently used SHM techniques include fiber optic sensors, piezoelectric or piezoresistive sensors, strain gauges and accelerometers to monitor the mechanical deformation, vibrations, or other parameters of the structure during the operation [13]ï [23]. However, most of these techniques can detect damage near its location therefore they must be placed near the critical zones on the structure. To counter this, sensors network systems had also been used to triangulate the location of the damage using lamb wave propagation, but the cost, size, and

weight of such a system limit their use not to mention the complex data processing required [24]. Moreover, SHM systems attached to the surface of the composites such as optical fibers and strain gauges had a drawback of being exposed to the environmental conditions for example, chemical, thermal, humidity, and external mechanical effect [25], [26]. Therefore, researchers are more focused on integrable monitoring sensors to not only monitor the overall deformation of the structure but to also monitor the internal behavior between the laminates of the composites. However, the insertion of the monitoring sensor entity in the composites is still underdeveloped and the prime focus is that it would not affect the performance of the composite structures. In previous studies, various sensors were developed and inserted inside the composites such as fiber Bragg grating, carbon nanotubes, carbon black, or carbon fibers [27]ï [32]. However, the use of optical sensors methods is limited because of the high cost to produce an optical fiber with fiber Bragg grating. Moreover, the use of nanomaterials as a damage sensing system is quite complex and expensive.

In comparison, carbon fibers (CF) used as a sensor because of their good electrical conductivity is a possible simple, durable, and cost-effective solution for damage monitoring in real-time [33]. CF consists of graphite-based microstructure and loading these fibers could deduce change in electrical behavior because of the change in their mechanical structure thus, depicting piezoresistive behavior [34]. Besides, the integration of CF in fiber-reinforced composites is quite easy because of the textile processing compatibility [35]ï [37]. The electromechanical response of Carbon fibers was first study by Concor and Owston [38] which showed that resistance of these fibers rises linearly with the applied strain and they also

studied their mechanical performance and contact resistance [35]. After these studies, continuous carbon fibers had been in use as self-sensing materials in composites because of simplicity in application, high mechanical performance and less cost [39]ï [46]. However, straightness of the filaments in the CF sensor plays a vital role to define the contact resistance and overall performance of the sensor[38], [44], [45].

In this experimental investigation, the real-time strain detecting ability of the CF sensor, consisting of unidirectional carbon filaments aligned together, was examined in chopped glass fiber reinforced polymer (GFRP) composites under tensile and flexural loading. The sensitivity of the CF to the applied strain was calculated experimentally by gauge factor (GF) calculation using a standalone sensor. Afterward, the general electromechanical behavior of the CF sensor was examined up to fracture to validate its response under large strain application or during any damage that was vital to comprehend its use in high strain applications. Then, this CF sensor was positioned in 0°, +45°, 90°, -45° directions through the plies gradually in a glass fiber reinforced polymer (GFRP) composites and the composite specimens were tested under tensile and flexural cyclic loadings. The results showed interesting behavior and presented that the CF sensor did not only detected and identified the strain under both loadings but also the intensity of the signal measured the amount of deformation. Moreover, the results demonstrated that the position and direction of the sensor plays a vital role in the detection and identification of strain by the sensor. This study would show the multimode detection of deformation in composites under different loading conditions using CF sensor over the large section and unapproachable locations

2. Fabrication Process

Carbon fibers (CF) consisted of unidirectional filaments of carbon produced at low-pressure vacuum from a precursor Polyacrylonitrile (PAN) polymer and this process is described in detail in [47]. Then, these unidirectional filaments were aligned together in specific length and width to be used as CF sensors for multimode strain monitoring in glass fiber reinforced polymer (GFRP) composites, Figure 1. The process of integrating CF sensors in their respective position and direction in a composite specimen for in-situ strain monitoring required electrical isolation of these sensors from each other and from the material itself. That is why, composite specimens were prepared using chopped glass fiber plies because of their high electrical resistance and non-conductivity and it also ensured the isotropic nature of the composite sample. Five plies of chopped glass fiber mat were used in a single composite specimen and each CF sensor was placed in its respective directions i.e. sensor A in 0°, sensor B in 45°, sensor C in 90° and sensor D in -45° and were separated by each ply. Then, resin and hardener mixture in a 1:4 ratio was poured into the mold and full incorporation of CF sensor in each position was achieved. Then, the sample was left at room temperature for 2 days for curing, and the sensor in each position was visible in all cured specimens. Then, each composite plate was cut into a star shape and each leg indicated the position and direction of the CF sensor, Figure 2a. The thickness of the composite specimen was kept as 5 mm and width and length of the individual leg of the star sample were kept at a standard measurement of 25 mm and 200 mm respectively, Figure 2b. Schematic illustration of the composite star sample integrated with the CF sensor showed that the sensor in each leg was represented by

sensors A, B, C, and D according to their reference direction and the position of each sensor within the plies of the sample, Figure 2c-2d.

(a)

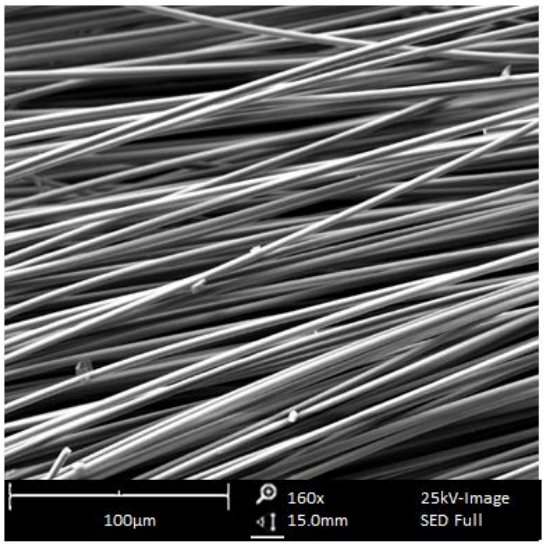

(b)

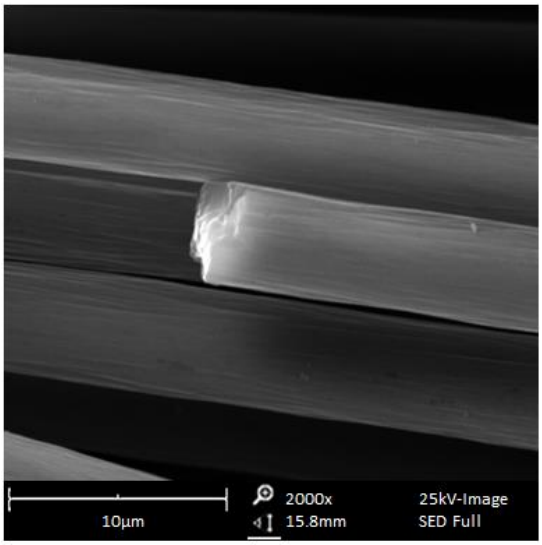

(c)

Figure 1: SEM images of the CF sensor. (a) PAN carbon fibers (b) SEM of unidirectional filaments of Carbon aligned together (c) magnified image to show the single fiber of carbon.

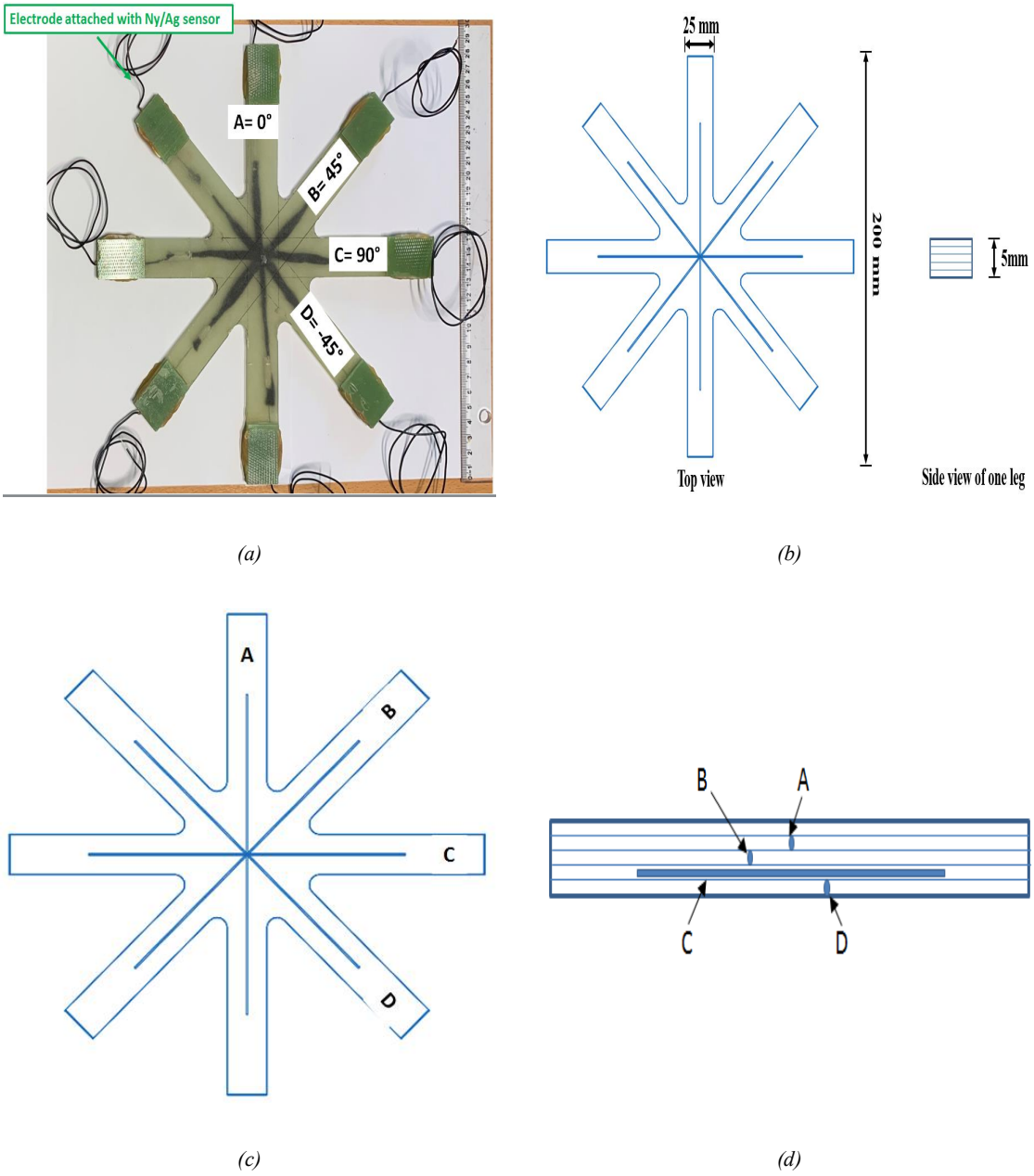

(a) *(b)*

(c) *(d)*

Figure 2: (a) Composite specimen integrated with CF sensor after the fabrication process and sensors are visible in each position as the specimen became transparent after the curing process. (b) Geometric specifications of the composite specimen. (c)-(d) Schematic illustration of the direction and position (section view) of CF sensor respectively

3. Experimentation

3.1. Experimentation of standalone CF sensor for GF calculation

CF sensor was tested under tensile load as a standalone sensor of 72 mm length and 0.5 mm

width using the INSTRON-50 apparatus. The data acquisition system was attached through electrodes at both ends of the CF sensor to simultaneously record the variation in the electrical resistance with the applied strain and calculate its gauge factor (GF). The sample was placed in the machine using a paper support as it was difficult to place the CF sensor alone between the fixture of the machine and before the start of the test, the paper frame was cut in the middle to not affect the mechanical response of the CF sensor during the test, Figure 3. Also, it was vital to ensure that the CF sensor was not in contact with any metallic part of the machine because it could influence its electrical response that is why, all the required parts of the machine were isolated by covering with the insulation tape. It should be kept in mind that the filaments in the CF sensor were unstrained when placed between the fixture before the test and there was no slippage between the electrode and sensor connection during the test as it was accurately and properly secured between the fixtures, Figure 4. Three successful tests were conducted with the CF sensor up to fracture to comprehend its electrical behavior with the variation in mechanical performance for high strain applications. The sensor was applied with tensile strain at a low strain rate of 2mm/min and the results showed repeatability in the response of the CF sensor.

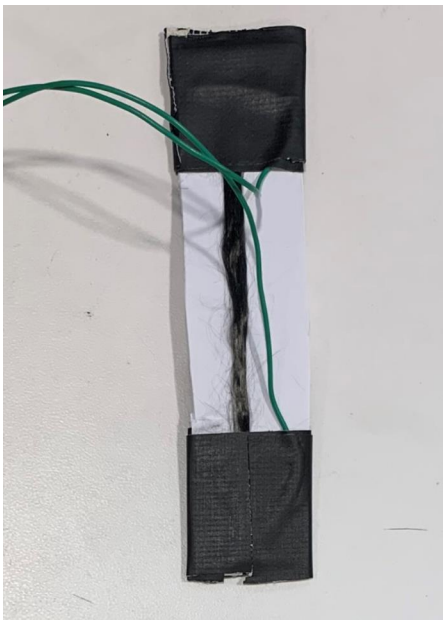

Figure 3: Preparation of CF sensor for standalone experimental test for the GF calculation. A set of papers are used as a support and electrode is attached on each end.

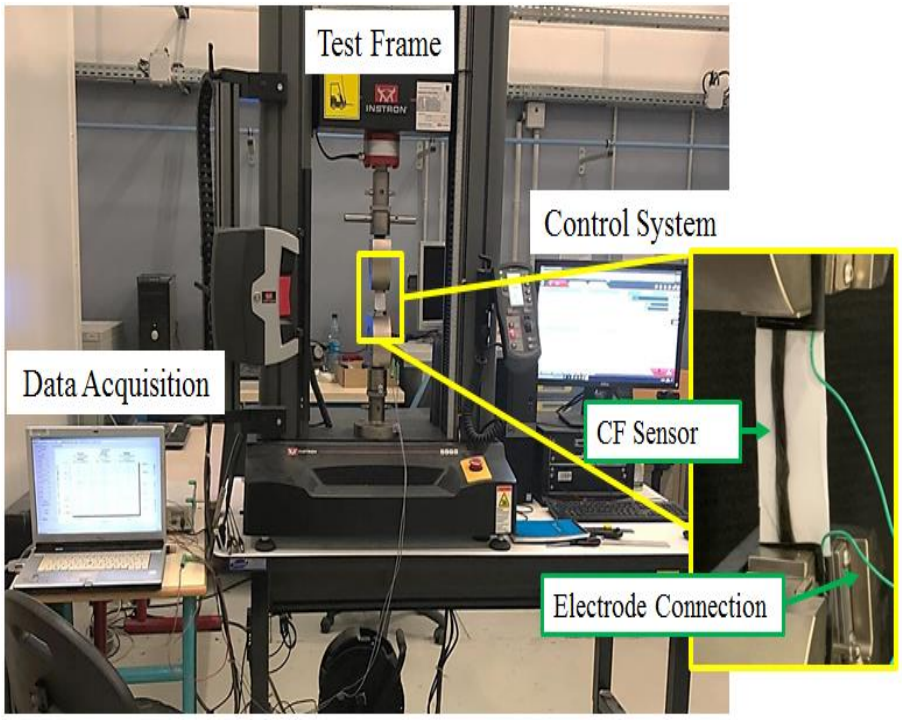

Figure 4: Experimental arrangement to examine the strain sensitivity of the CF sensor.

3.2. Experimental testing of composite integrated with CF sensor

Composite specimens instrumented with CF sensors in different direction and position was tested using INSTRON-50 and data acquisition system was attached to each sensor using electrodes for real-time monitoring of strain deformation. INSTRON-50 recorded the mechanical performance of the composite sample and the data acquisition system simultaneously recorded the response of each CF sensor. Two sets of tests were performed on the composite star specimens. The first set of tests included the study of three composite specimens under tensile cyclic loading and the second test was included the testing of three-star specimens under cyclic flexural loading to understand the real-time monitoring response of the CF sensor in detail, Figure 5. In both tests, it was important to place the sample properly among the fixtures and to isolate the electrical connections from any metallic portion of the machine near. Moreover, the shape of the specimen made it easier to place it between the fixtures during the tensile cyclic loading but the placement of the specimen between the rollers of the flexural cyclic test was a bit difficult. That is why, the strain rate for the tensile test was kept 5 mm/min applied up to 15 kN and for flexural test it was kept 2 mm/min applied up to 2kN to ensure no permanent deformation in the samples. All tests were performed for 10 cycles and it must be noted that the range of strain rate in quasi-static tests is so low that it does not affect the mechanical behavior of the sample or the electrical response of the sensor [48]. Each test presented that the CF sensor in each position and direction showed a distinct resistance profile in both sets of tests which will be discussed in detail in the next section.

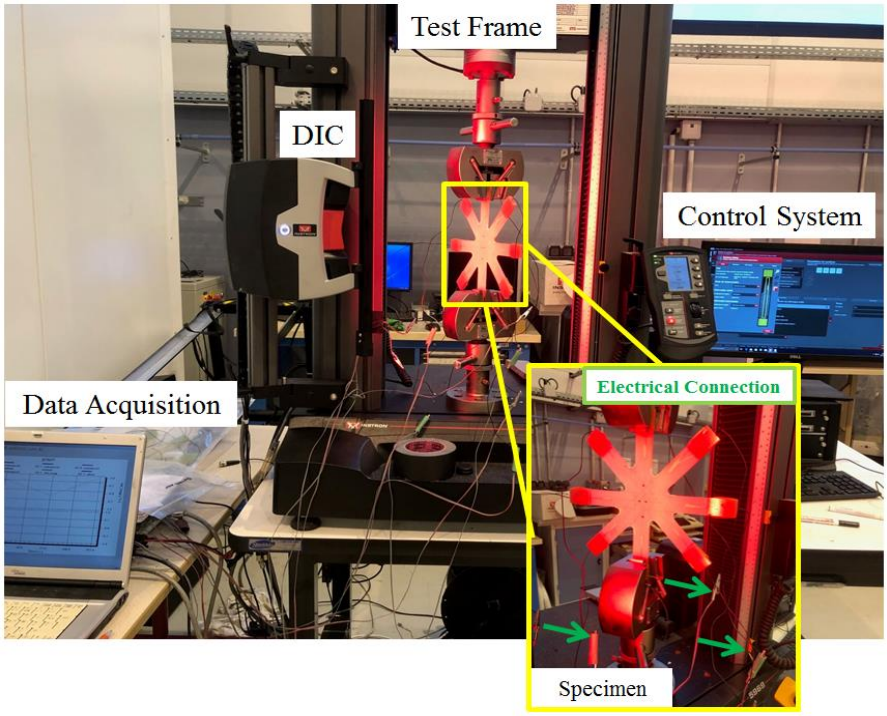

(a) Tensile test setup

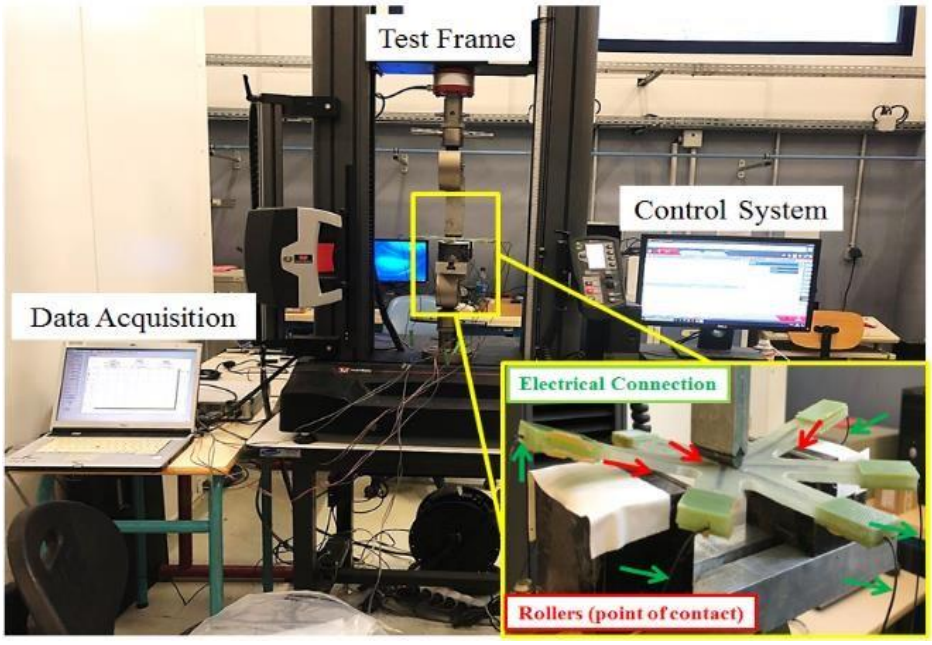

(b) Three-point bend test setup

Figure 5: Experimental arrangement to examine the real-time strain monitoring response of CF sensor in composites.

4. Mechanical properties of CF sensor

4.1. Mechanical Characterization

The CF sensor displayed good mechanical behavior and the Young's modulus and yield strength of all the examined CF sensor samples were about 94.53 MPa and 1.73 MPa respectively on average during the standalone test, Figure 6a. Table 1 summarizes the mechanical behavior of the CF sensor, consisting of yieldôs strength, Young's modulus, and fracture strain. In overall mechanical behavior each sensor sample exhibited linear elastic deformation before the start of final fracture because of the high stiffness and CF sensor did not show any plastic deformation however, reduction in mechanical behavior was gradual due to the consecutive breakage of the filaments. Even though CF sensor showed high stiffness, but it was quite flexible because carbon filaments were held together loosely together and were combined only in the both ends were electrodes were attached. Therefore, these sensors could be used in high strain applications without compromising its mechanical performance, Figure 6b. Furthermore, it was observed that the damage initiation and propagation were not sudden, and the membrane was fractured gradually with the breakage of each filament.

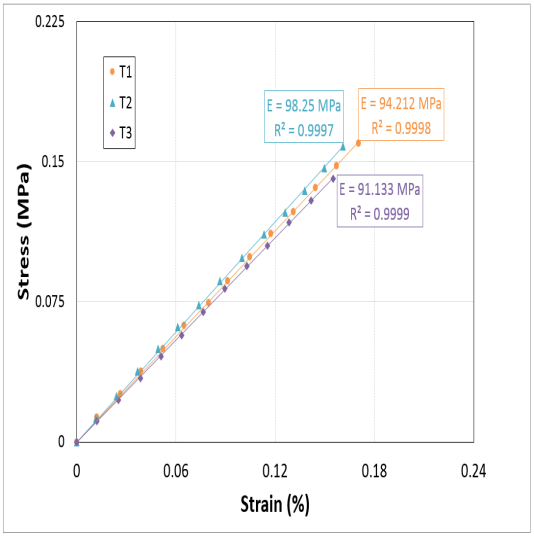

(a) Elastic Modulus

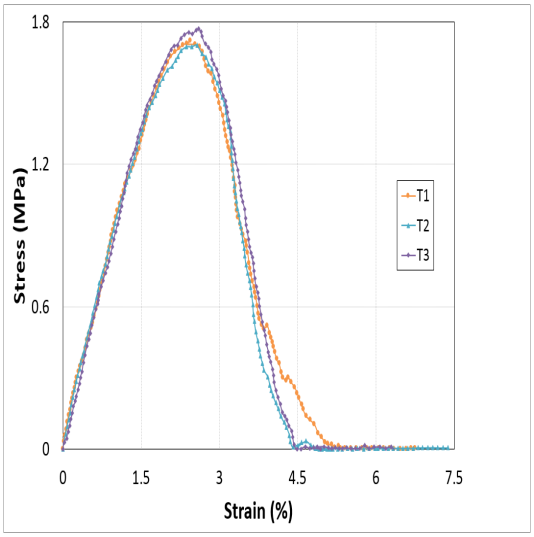

(b) Overall mechanical behavior

Figure 6: Mechanical performance of CF sensor.

Table 1: Mechanical properties of CF sensor under tensile loading

	Elastic Modulus (MPa)	**Fracture Strain (%)**	**Yield Strength (MPa)**
Sample 1	94.212	5.156	1.72
Sample2	98.247	4.44	1.70
Sample3	91.133	4.49	1.77
Average	94.53	4.46	1.73
Standard deviation	3.5677	0.0354	0.0360

4.2. Strain sensitivity

The resistance of the CF sensor was increased with the applied tensile strain which verified good correlation among its electromechanical response, Figure 7a. The sensitivity of the CF sensor was demonstrated in terms of GF by comparing the variation of resistance with the amount of applied tensile strain and calculated by using equation (1).

$$GF = \frac{\left(\Delta \frac{R}{Ro}\right)}{\varepsilon} \quad (1)$$

In this equation, $\Delta R/R_o$ is a main constituent to define the sensitivity of the CF strain sensor as

it signifies the ratio of original resistance to the variation of resistance with the applied strain ε. The GF of this sensor was calculated to be inside 10.2-10.8 range within the elastic limit, Figure 7b. it was confirmed that from these results the CF sensor had good strain sensitivity range and might be used for instantaneous strain monitoring of structures.

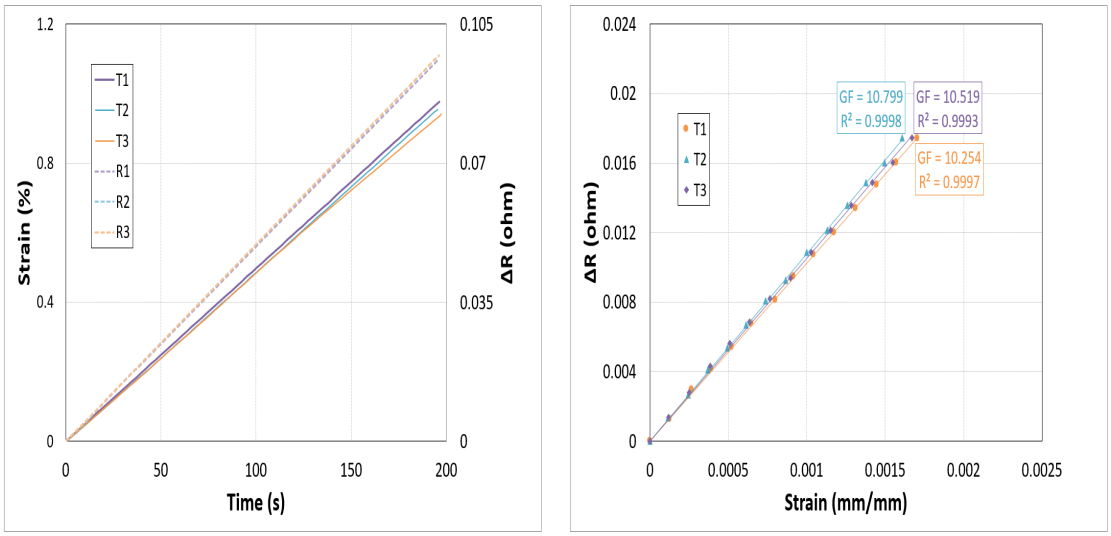

(a) Strain and resistance change in CF sensor during elongation

(b) GF calculation

Figure 7: Experimental behavior and calculation of the strain sensitivity of the CF membrane sensor

Each specimen of the CF sensor presented good electrical behavior throughout the applied tensile strain, resistance changed gradually, and all samples displayed similar overall performance. The overall behavior of the CF sensor presented that, during elastic behavior the change in resistance was linear, and when the mechanical behavior of the sensor started to degrade there was a sudden increase in the resistance which reached maximum value upon fracture of the membrane, Figure 8. Furthermore, the sudden increase in the resistance of the

sensor with the degradation of the mechanical behavior was progressing gradually to the maximum value because the carbon filaments in the sensor were breaking individual with the elongation, and with each breakage the resistance showed variation. the linear increase during the plastic deformation of the CF sensor. Moreover, an increase in resistance is directly proportional to an increase in the length (elongation) of the sensor, equation (2)-(3).

$$\alpha = \frac{1}{\rho} \tag{2}$$

$$R = \frac{\rho L}{A} \tag{3}$$

Where α is electrical conductivity, ρ is resistivity, L *is* length, A is the cross-sectional area, and R is resistance.

Also, it was observed in all specimens that the increase in resistance became more prominent when the mechanical strength of the sensor was reaching the minimum value which confirmed its ability to use for real-time strain monitoring application during high strain deformation of structures because the sensor showed good electrical conductance until all the filaments in it were broken.

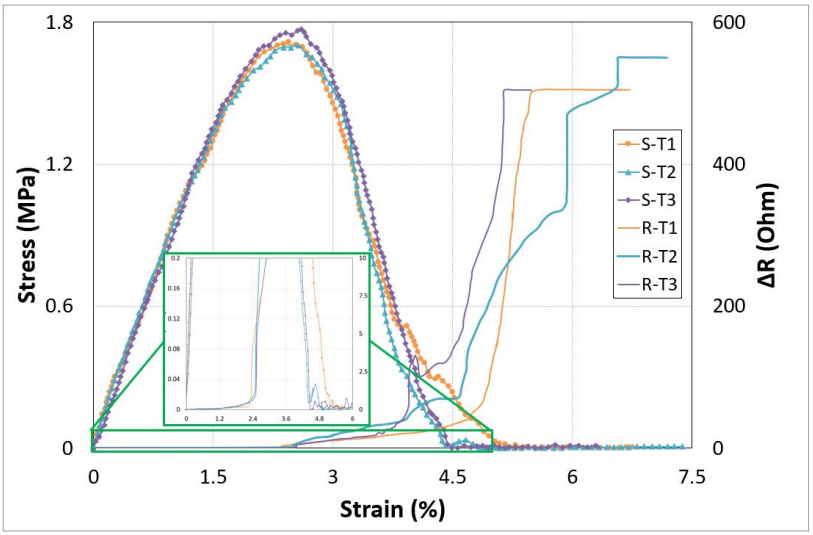

Figure 8: Overall electromechanical response of CF sensor specimens.

5. Real-time strain monitoring application of CF sensor

5.1. Strain monitoring in composites during cyclic tensile loading

First, it is important to understand the strain deformation of the composite under cyclic tensile loading to apprehend the strain detection by the CF sensor, Figure 9. One leg of the star specimen was fixed between the fixtures of the machine and the other legs were free. The loading axis was considered as the reference and sensor place in this direction was at 0° and labeled as sensor A. When the specimen was loaded, tensile stresses were produced in 0° and compression stresses were produced in 90° i.e. transverse direction. In addition, it was understood that the combined effect of tensile and compression stresses is generated in oblique direction i.e. $\pm$45°. However, in test 1 and 2, samples were placed between the fixtures in such manner that the leg of the star sample consisting of sensor A was along the loading axis i.e. in 0° and test 3 sample was placed in a way that the leg of the composite sample consisting of sensor C was along the loading axis i.e. in 0°, sensor A in 90° and sensor B & D interchanged their position, Figure 10. The step to interchange the positions of the CF

sensor in test 3 was conducted to examine the load sensitivity of the CF sensor and it didnôt affect the comparison of the mechanical performance of the composite samples. Three composite specimens were tested successfully, and mechanical behavior was plotted as elastic modulus and overall initial stress-strain curve which showed good repeatability in the behavior, Figure 11. Results confirmed that the mechanical behavior of all composite samples was similar irrespective of the choice of the loaded leg, was isotropic because of the use of the chopped glass fiber mat, and presence of CF sensor at different directions and positions did not affect the structureôs integrity.

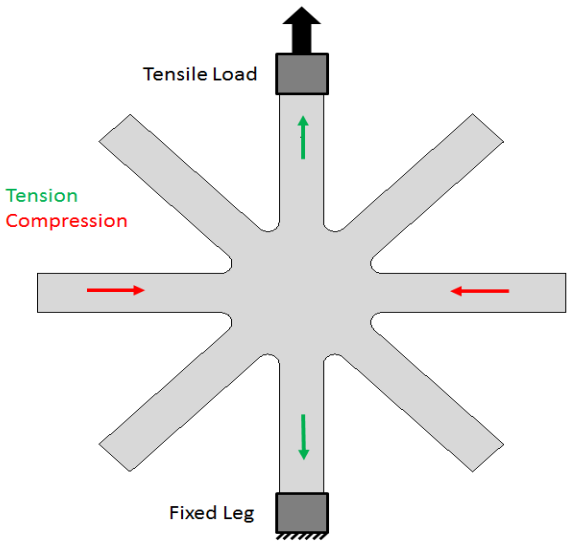

Figure 9: Deformation mechanism of the specimen during the applied tensile strain.

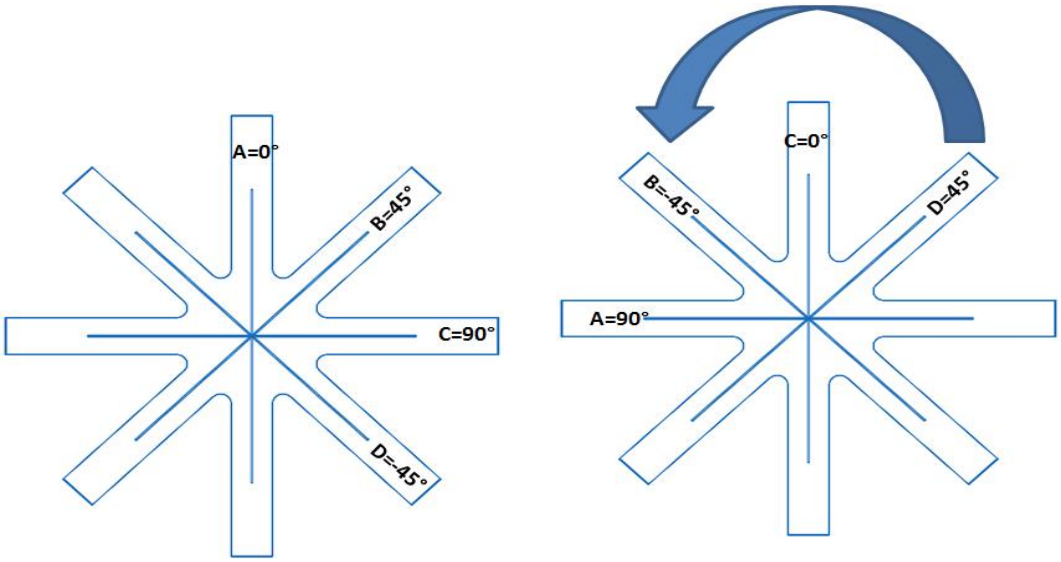

(a) Samples position in test 1 and 2 *(b) Sample position in test 3*

Figure 10: Placement of the composite sample between the fixtures of the tensile machine

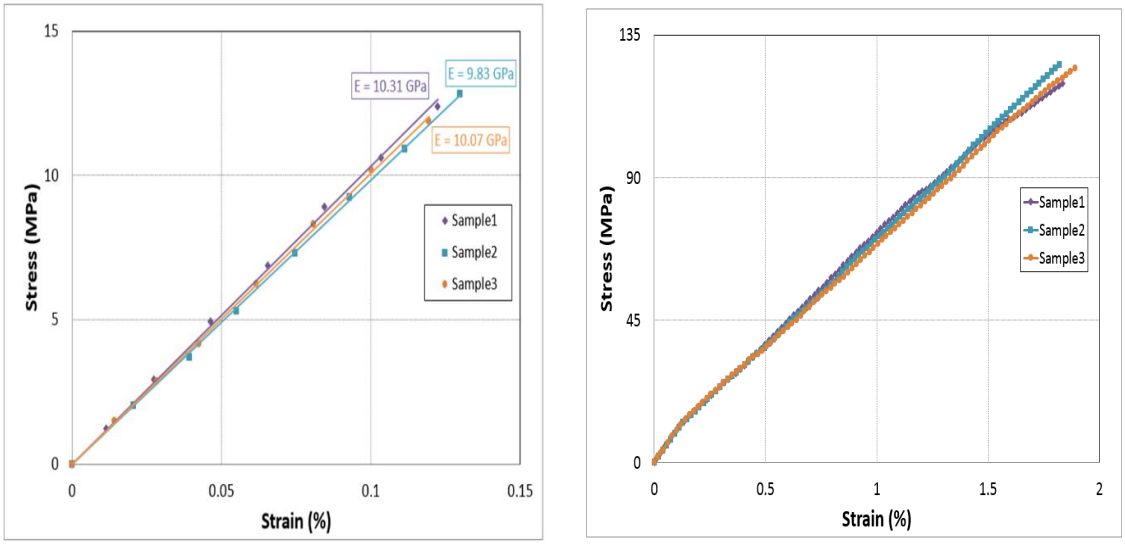

(a) Youngôs modulus *(b)* Overall initial stress-strain behavior

Figure 11: Mechanical performance of the composite star sample.

Flexible CF sensor displayed good electrical variation during the strain deformation of composite specimens in all three experimental tests. The resistance of CF sensor in each composite sample showed gradual change during each cycle of applied strain and showed

similar behavior in each direction. However, the electrical resistance of CF sensor within a single specimen showed difference intensity in the change of the signal with the applied strain because of their specific direction i.e. 0°, ±45°, 90° against the loading axis. This showed that the CF sensor did not only monitor the strain but also showed the amount of strain induced in each direction against the applied load. Moreover, consistency of the recorded signal during all 10 cycles showed the stability, durability, and integrity of the CF sensor.

- Tests 1 and 2 were performed to further confirmed the repeatability in the behavior of the CF sensor when produced in different batch. All the sensors A, B, C, and D presented variation in resistance according to the intensity of the deformation in their direction and correlated perfectly in both tests and each cycle, Figure 12. Furthermore, sensor A demonstrated the maximum change in its resistance when subjected to the cyclic loading that established the presence of maximum deformation of the sample in the loading direction because of the tensile elongation. Then, sensor B and D presented less variation in their resistance during the cyclic strain in comparison with sensor A because of their direction. Moreover, sensor place in B and D direction displayed an identical change in resistance which is because these two positions were the mirror of each other regarding the loading axis and they confirmed the isotropic nature of the material. CF sensor in position C showed minimum variation in the resistance due to its transverse direction regarding the loading axis. This change was positive however, negative change was expected because of the compressive stresses, to justify the Poisson's effect under tensile loading. This positive change could be because of the complex interaction between the

laminar stresses and the conduction behavior of the carbon filaments in the CF. As discussed before, the filaments are loosely aligned together in one direction and were only attached in the ends in the conductive membrane. The compression strain in the transverse direction could indeed cause the decrease in length of the sensor which would result in the decrease in its resistance but, this compression might cause the increase in the contact distance between the loosely aligned filaments of CF sensors and this could be further facilitated by the tensile elongation in the middle of the specimen where all sensors are passing through the center. That is why the sensor in the transverse direction showed minimum but positive change in the resistance.

- Sample 3 was tested and compared with the results of Sample 1 to test the load sensitivity of the CF sensor, Figure 13. In test 3, sensor C recorded the maximum change in the resistance during the cyclic tensile load because of its position along the loaded axis and sensor A showed detection of minimum strain deformation because of its transverse position regarding the loading axis. However, CF sensors placed in B and D showed an identical change in the signal because of their similar direction according to the loading axis in both tests 1 and 3 i.e. $\pm$45°. Moreover, it was observed that the intensity of the change in signal of the CF sensor in a particular position was similar in both cases i.e. test 1 and 3 regardless of sensor label. For instance, sensor A in test 1 and sensor C in test 3 showed almost equal intensity of the increase in resistance with the applied strain because of a similar position with minor variation. Similar behavior was observed for the rest of the position which confirmed that the position of the sensor plays a key part in not only

detecting the deformation but also identify the amount of strain produced in the respective direction. Thus, this confirms the sensitivity of the sensor is dependent on their location according to the loading direction, Figure 14.

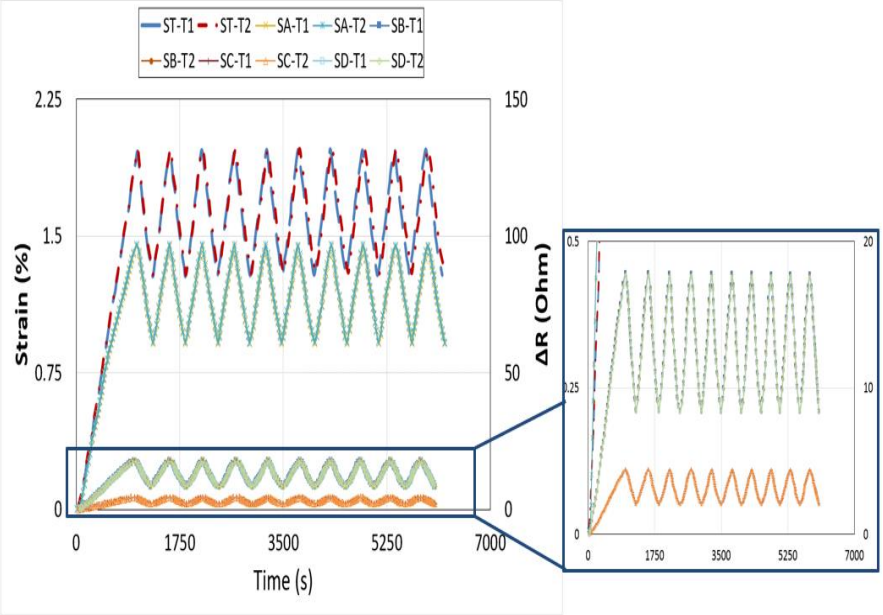

Figure 12: Real-time tensile strain monitoring in the composite specimen by CF sensor and verification of the test reproducibility

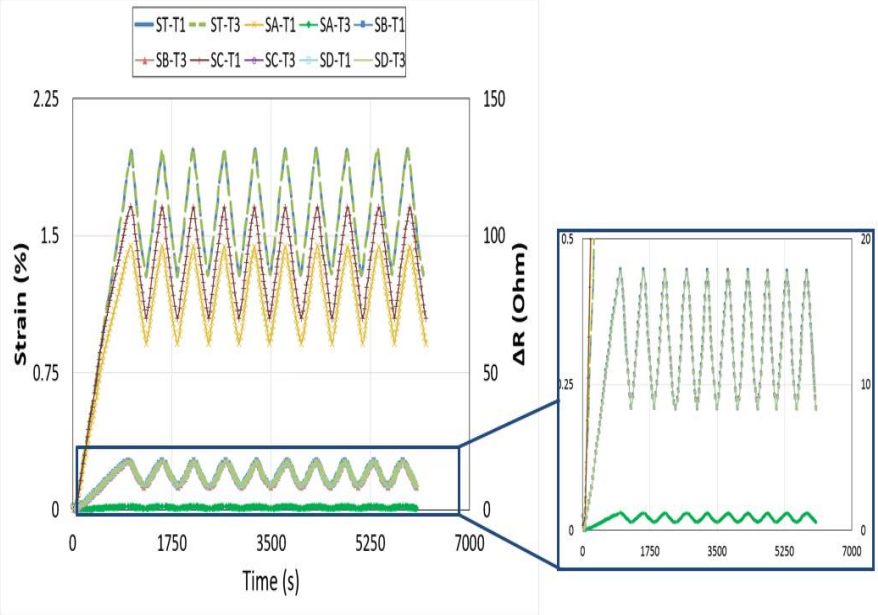

Figure 13: Comparison of real-time strain monitoring of composite star specimen by CF sensor during test 1 (when sensor A is placed in loading direction) and test 3 (when sensor C is placed in loading direction)

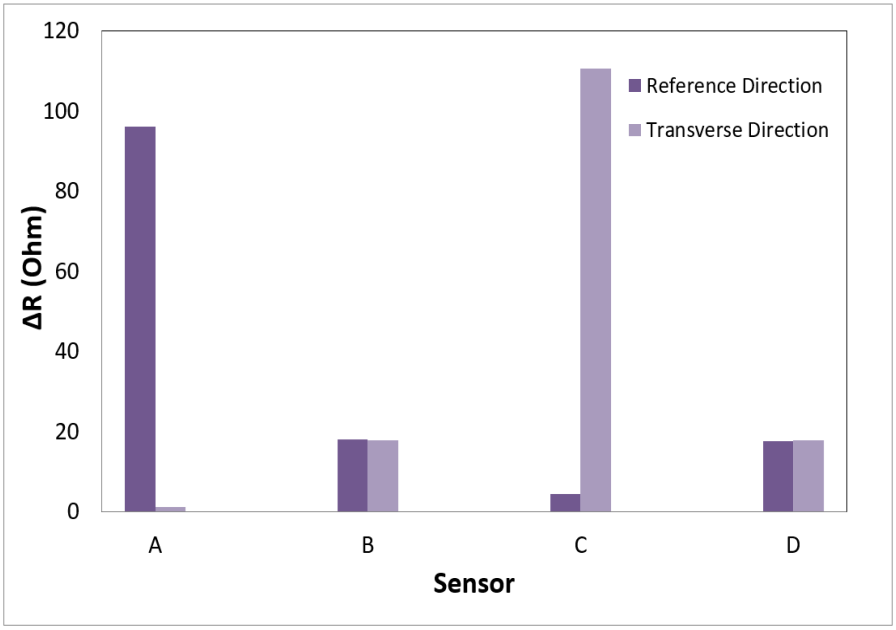

Figure 14: Effect of position and direction on the sensitivity of the CF sensor regarding the applied load.

5.2. Strain monitoring behavior in composites during cyclic flexural loading

Like the tensile test, it is also significant to comprehend the flexural strain of the composite sample during the three-point bend test to apprehend the response of the CF sensor during the detection of flexural strain. Star specimen was placed in the machine for a three-point bend test in such a manner that one leg of the star sample was loaded among three-roller fixtures while all other legs were free. The loaded leg was positioned as a simply supported beam on the bottom two rollers and force and deflection were applied by the upper roller at the center of the span length, Figure 15a. Moreover, it should be kept in mind that in all three tests, the star sample was positioned among the rollers in such a manner that sensor A was in the roller axis direction and the sensor C was in the loaded leg i.e. within the span length. Once the

sample was deflected during the three-point bend test, it was deformed within the span light and there were compressive strain (shown by green) at the top surface because of the compressive force of the roller and tensile strain near the bottom of the sample because of the tensile elongation(shown by red arrows), Figure 15b. Then these tensile strain (from bottom) and compressive strain (from top) propagate through each ply which could result in sample failure. It should be kept in mind that during flexural bending the load was applied perpendicular to the sensor arrangement unlike in the tensile test where the loading axis was aligned with the sensor arrangement.

Three samples were tested in such a manner that samples in tests 1 and 2 were placed between the rollers with sensor A in the top position within the roller axis (Case I) and sample in test 3 was placed between the roller with sensor D in the top position and sensor A in the bottom position (Case II) while sensor C was along the span length in both cases, Figure 16. This step was carried out to study the position sensitivity of the CF sensor and its capacity to sense strain deformation within the plies of the composite during flexural deflection. Mechanical behavior under flexural loading was calculated using equation (4)-(6) and results showed that inverting the positions of the sensors did not affect the mechanical behavior of the composite with good reproducibility, Figure 17. This further established that the presence of flexible CF sensors in different positions and directions did not affect the overall mechanical performance, structural integrity, and isotropic nature of the star specimen[8].

$$\sigma_f = \frac{3FL}{2bd^2} \tag{4}$$

$$\varepsilon_f = \frac{6Dd}{L^2} \tag{5}$$

$$E_f = \frac{L^3 m}{4bd^3} \tag{6}$$

Where, σ_f is the flexural stress, ε_f is the flexural strain, E_f is the flexural modulus of elasticity, F is the load, L is the span length, b is the width, d is the thickness, D is the deflection, and m is the slope of the load-deflection graph.

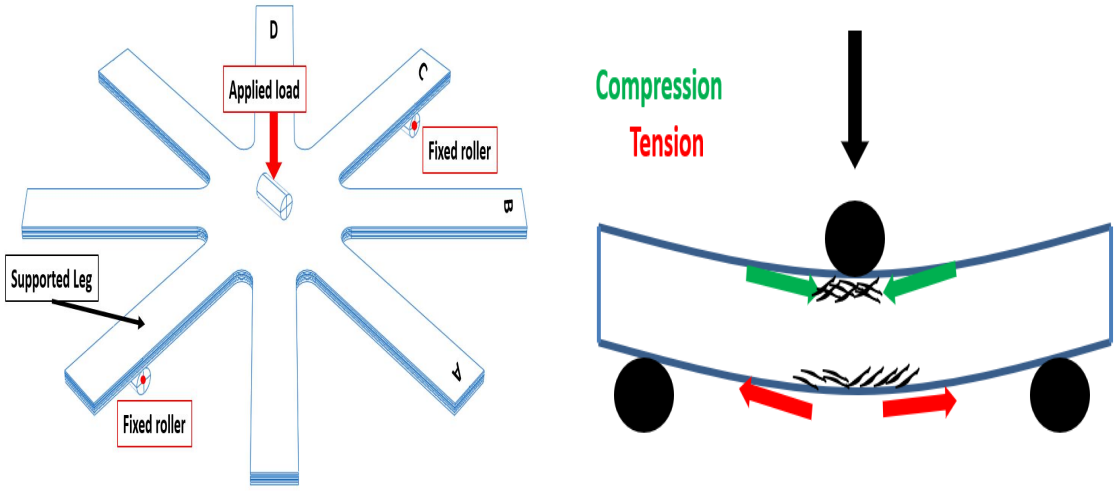

(a) Specimen placed between the roller fixtures in the machine *(b) Deformation behavior of the specimen*

Figure 15: Mechanical strain deformation of composite star sample during flexural loading.

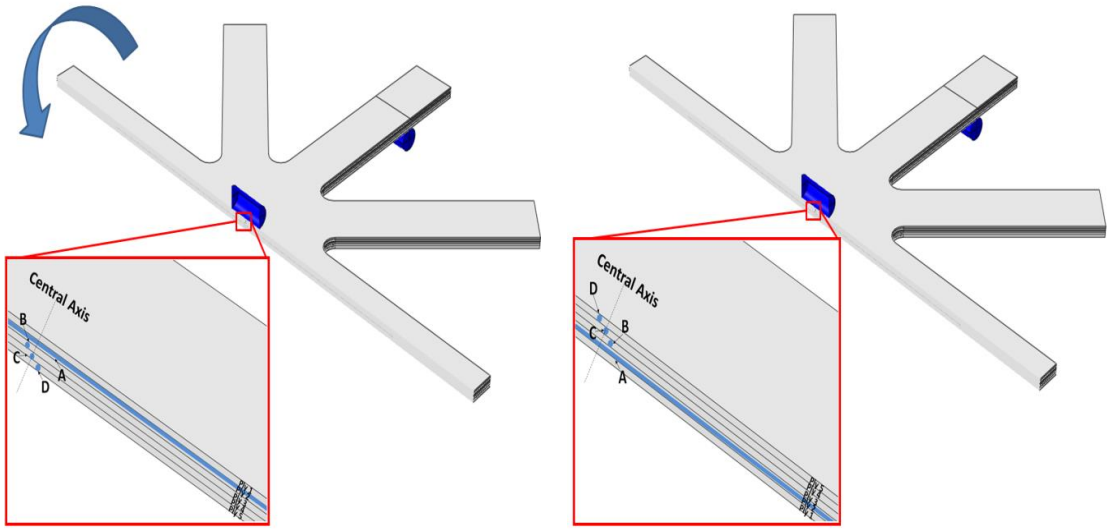

(a) Case I *(b)Case II*

Figure 16: Position of the star specimen between the three rollers fixtures for flexural bending: (a) Samples placed during test 1 and 2 when sensor A is in top position and sensor D is in lowest position (b) Sample placed during test 3 when sensor A is in the lowest position and sensor D is in top position. Sensor C is in the loaded leg during all three tests.

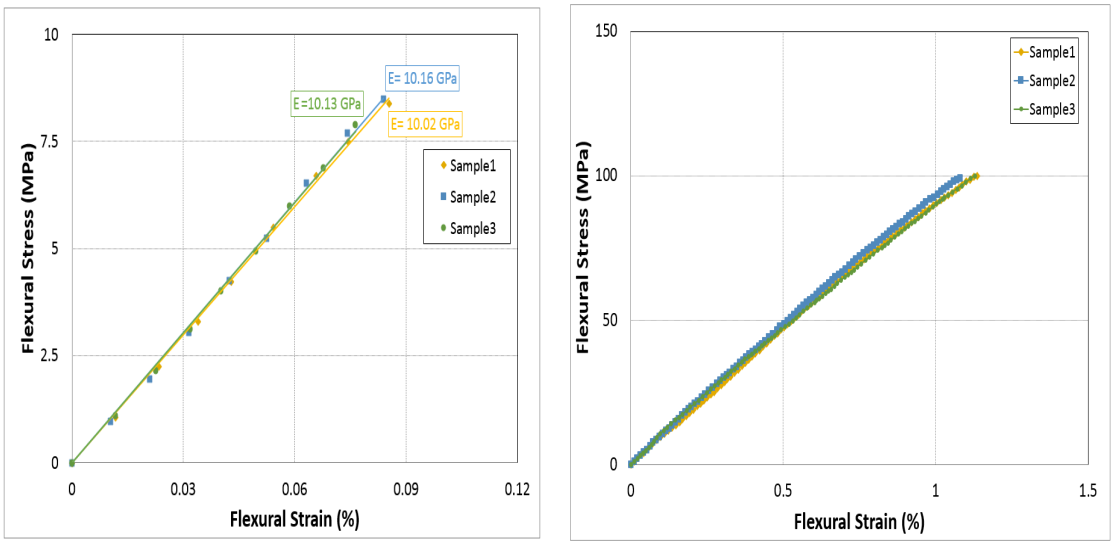

(a) Young's modulus *(b) Overall initial flexural stress-strain behavior*

Figure 17: Mechanical behavior of all three star-samples during flexural deflection.

The change in electrical resistance of the CF sensor was gradual with the applied strain during the flexural deflection with good repeatability in results during each cycle. CF sensors showed a distinct change in behavior according to their respective direction according to the roller axis and location between each plie (through-thickness). As discussed before, Sample 1 and 2 were tested with sensor A in the top location and aligned with the roller axis to demonstrate the repeatability in the response and real-time strain monitoring of the CF sensor when prepared in different batch. CF sensors in all four positions showed a gradual change in their resistance and correlated perfectly with the applied strain, Figure 18. Moreover, it was observed that CF sensors showed a positive change in resistance placed below the neutral axis and negative change in resistance placed above the neutral axis of the specimen during the bending. Test 3 was performed to test the position sensitivity of the CF sensor with the loading axis (perpendicular to the specimen) in which sensor A was in the bottom position and positions of the other sensors were changed accordingly, Figure 19. Even in test 3, CF sensors i.e. sensor C and D in two positions above the neutral axis showed a decrease in resistance and sensor A, B in two positions below the neutral axis showed an increase in resistance during the cyclic flexural load. Moreover, each sensor showed the different intensity of variation in resistance whether positive or negative thus, quantified the amount of damage induced in each direction and position.

In both cases, the CF sensor in all four positions showed distinct performance which was required to be discussed in detail consecutively to comprehend the in-situ detection of deformation during the flexural bending by CF sensor in each position.

- Sensor A: was in 0° direction regarding the roller axis and was positioned on top in case I and in the bottom in case II. It must be noticed that this leg of the star sample wasnôt loaded directly but was solitary under the indirect influence of the flexural load applied by the top roller in both cases. Sensor A detected a maximum decrease in resistance in case I while in case II, when it was in the bottom position, it detected a maximum increase in resistance with maximum strain deformation, Figure 18. This confirmed that the CF sensor was able to detect the compression strain induced by the roller which was in direct contact with the upper surface. The localized direct contact between the upper and surface of the composite and roller resulted in the generation of maximum compression strain thus, sensor A showed a maximum decrease in resistance. This behavior was different from the strain detection during the tensile test because during flexural the load is applied perpendicular to the sensor arrangement and it could decrease the contact distance of the loosely aligned carbon filaments of the sensor CF. In case II, sensor A was placed near the bottom surface where the sample experienced tensile elongation and it showed a maximum increase in resistance in comparison to the other sensor in other positions. This showed that it was able to detect the strain in the bottom case and to identify it as the tensile elongation. Moreover, the intensity of the signal showed the amount of damage induced, Figure 19.
- Sensor B: was in +45° in case I and in -45° in case II regarding the roller axis while it was situated second from the top in former and second from the bottom in latter case i.e. between ply 2 and 3 and near the neutral axis of the specimen. This leg of the star sample was not under the direct impact of the flexural load as well but only under the localized

influence of the central roller. In tests 1 and 2, sensor B showed good reproducibility in results and correlated perfectly with the applied strain in each cycle, Figure 18. The behavior of the signal of sensor B was similar to the sensor A but, the intensity of the change in the detection signal of sensor B in comparison to sensor A was decreased in both cases as it was closer to the neutral axis. In comparison between test 1 and test 3, it was observed that the intensity of the signal of CF sensor change because of the change in the position, Figure 19. Sensor B show good detection of minimum compression strain in case I and minimum tensile strain in case II because it was not only near the neutral axis of the specimen but also under the indirect influence of the bending load as it was not in the loaded leg of the star sample, Figure 20.

Å Sensor C: was in 90° direction regarding the roller axis in both cases I and II and in the leg of the star specimens placed between the rollers, along the span length and between the 3rd and 4th ply. This leg of the star sample was the one section in addition to the center of the specimen which was fully under the effect of bending deflection in both cases. During test 1 and test 2, the CF sensor as sensor C showed maximum intensity in the detection signal in comparison with all the other sensor positions and correlated perfectly in each cycle of the applied strain, Figure 18. This is because it was placed within the loaded leg of the star sample and was under the maximum influence of the flexural deflection and even though it was close to the neutral axis it showed maximum increase in resistance in comparison with sensor D which was placed near the bottom. Moreover, sensor C detected the tensile strain by showing the increase in resistance with applied deflection in each cycle, and this

detection was not localized but along the whole span length. However, in case II when the position of sensor C was change and was above the neutral axis, it showed a maximum decrease in the resistance because of the presence of compression strain and the detection was along the whole span length, Figure 19. So, this showed that even though the position of sensor C was near the neutral axis of the sample like sensor B but, it showed the maximum intensity of the signal in both cases in comparison with sensor D because of its presence along the span length of the sample and covering the larger area for detection of deformation, Figure 20.

Å Sensor D: was in -45° direction in case I and 45° direction in case II regarding the roller axis and was in the bottom position in the former case and the top position in the latter case. This leg of the composite star sample was also not under the direct effect of flexural deflection but only under the localized influence of the central roller. During test 1 and test 2 (case I) in both star specimens, sensor D showed repeatability in detection signal and correlated with the applied strain in a good manner, Figure 18. In case I, sensor D showed the minimum increase in resistance of the signal in comparison with sensor C and other sensors even though it was placed near the bottom of the specimen where it detected only localized tensile elongation during the deflection of the specimen between the rollers and sensor C was along the span length in the loaded leg and under the direct influence of flexural bending as discussed before. In case II, sensor D showed a decrease in the resistance because of the localized compression strain produced by the upper roller however, it was less than the sensor C because of the position along the span length, Figure

19-20.

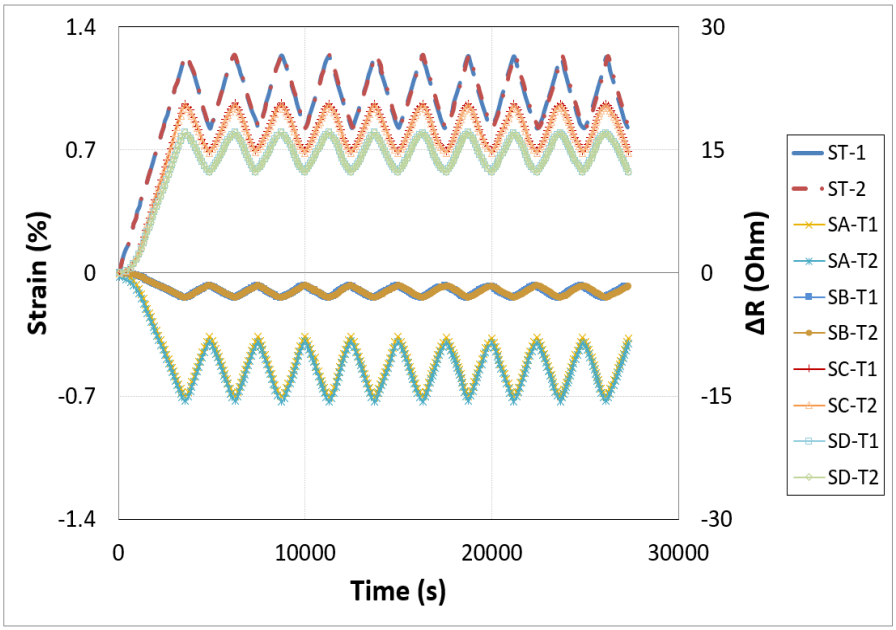

Figure 18: Real-time strain monitoring in composite star specimen during cycle flexural bending using CF sensor

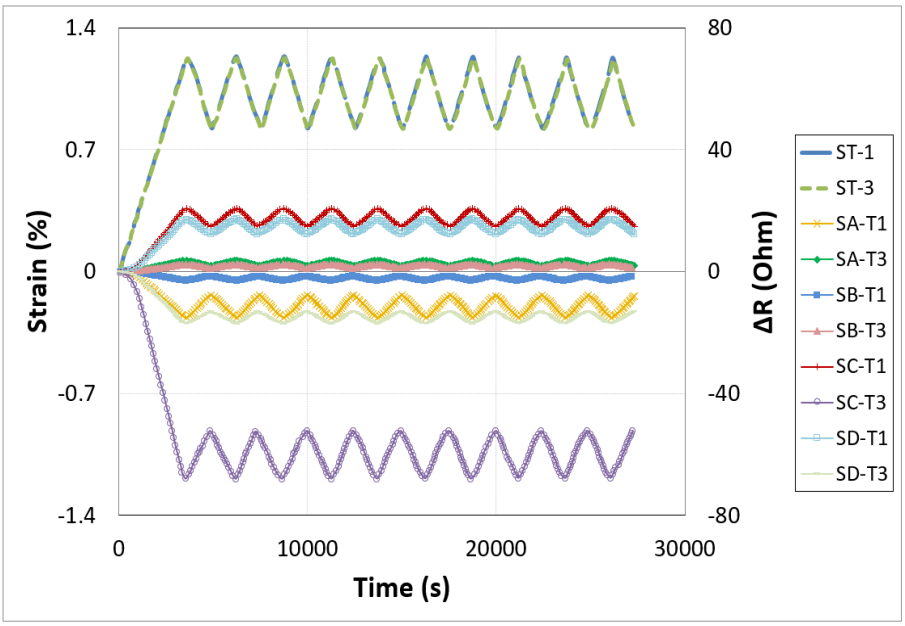

Figure 19: Comparison of real-time strain monitoring behavior of CF sensor in composite star specimen during cycle flexural bending during test 1 (when sensor A is placed in top position according to the loading axis) and test 3 (when sensor A is placed in bottom position according to the loading axis).

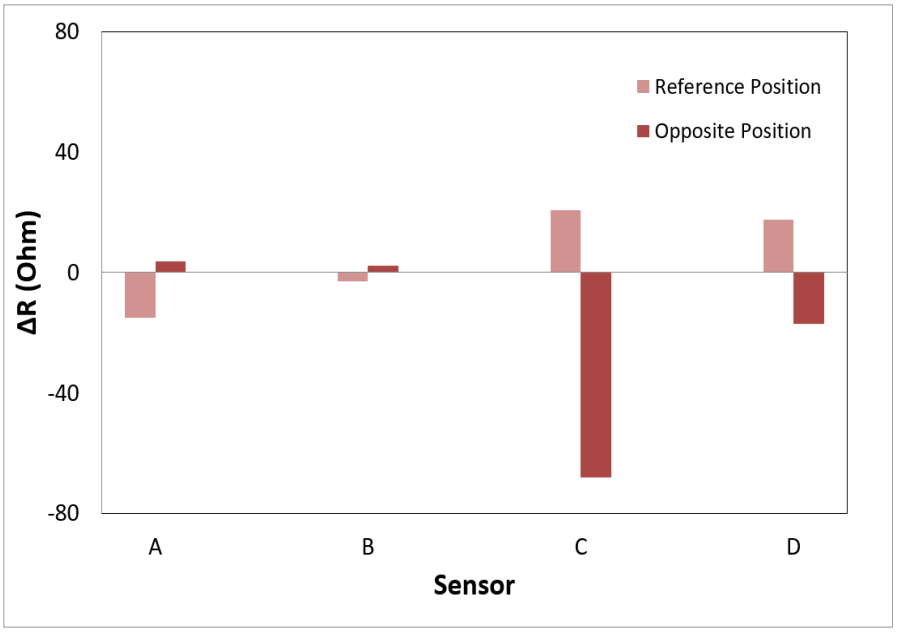

Figure 20: Effect of position and direction on the sensitivity of the CF sensor against the loading axis and position through-thickness.

6 Conclusions

The objective of this extensive experimental study was to develop a simple, robust, and cost-effective sensor system with high electrical conductance for multimode real-time strain monitoring in composites during different loading conditions. This CF sensor showed viable replacement of conventional strain gauges and SHM systems. These sensors showed high sensitivity to applied strain in the range of 10.2-10.8, were more flexible, and could be easily integrated within the composite specimens. The method of placing these sensors in different directions and positions showed that these sensors can detect deformation over large areas and sections of complex structures and in locations that are not normally accessible to conventional methods. The study of real-time monitoring of strain by CF sensor under tensile and flexural cyclic loads demonstrated the behavior of detection signals in detail. Monitoring

of deformation under tensile strain showed the influence of the direction of CF sensor regarding the loading axis on the change in resistance while monitoring of deformation of the composite specimen under flexural bending showed the influence of the position of the sensor within the plies on the detection signal of the CF sensor when the load is applied perpendicular to the arrangement of the sensors. Results confirmed that CF sensors in both tests reacted to the applied stimuli in every direction and showed a distinct change in their change in resistance. CF sensor was able to detect and identify the type of strain under flexural loading when the load was applied perpendicular to the sensor arrangement but during tensile loading, it was unable to show a decrease in resistance in the transverse direction because of increase in contact distance between the loosely aligned carbon filaments when the load is applied along the plane of the sensor arrangement. So, in general, it not only monitoring the deformation but also detecting the type of deformation whether tensile or compressive, and quantified the amount of damage induced in each position and direction within the composite sample. However, further study is required to understand the precise mechanism responsible for changing the resistance of the sensors to apprehend its response in the transverse direction or under compression strain during tensile loading. Additional understanding could make it possible to tailor the arrangement of filaments in the CF sensor so that the behavior of the sensor is predictable under both loading i.e. tensile and compression. This sensor technology can further advance itself in the real-time sensing applications within composite structures including thermal degradation and detection of dynamic failure. The sensitivity of this sensor can be further tailored and amplified as desired

parameters by modifying the arrangement or alignment of carbon filaments and without any significant requirements.

References

[1] F. Axisa, P. M. Schmitt, C. Géhin, G. Delhomme, E. McAdams, and A. Dittmar, ñFlexible technologies and smart clothing for citizen medicine, home healthcare, and disease prevention,ò *IEEE Trans. Inf. Technol. Biomed.*, vol. 9, pp. 325ï 336, 2005.

[2] C. Simon, E. Potter, M. McCabe, and C. Baggerman, ñSmart fabrics technology development,ò 2010.

[3] S. Sassi, M. Tarfaoui, and H. B. Yahia, ñThermomechanical behavior of adhesively bonded joints under out-of-plane dynamic compression loading at high strain rate,ò *J. Compos. Mater.*, vol. 52, no. 30, pp. 4171ï 4184, 2018.

[4] H. Benyahia, M. Tarfaoui, A. El Moumen, D. Ouinas, and O. H. Hassoon, ñMechanical properties of offshoring polymer composite pipes at various temperatures,ò *Compos. Part B Eng.*, vol. 152, pp. 231ï 240, 2018.

[5] K. Diamanti and C. Soutis, ñStructural health monitoring techniques for aircraft composite structures,ò *Prog. Aerosp. Sci.*, vol. 46, no. 8, pp. 342ï 352, 2010.

[6] L. C. Hollaway, ñA review of the present and future utilisation of FRP composites in the civil infrastructure with reference to their important in-service properties,ò *Constr. Build. Mater.*, vol. 24, no. 12, pp. 2419ï 2445, 2010.

[7] O. H. Hassoon, M. Tarfaoui, and A. E. M. Alaoui, ñAn experimental investigation on dynamic response of composite panels subjected to hydroelastic impact loading at

constant velocities,ò *Eng. Struct.*, vol. 153, pp. 180ï 190, 2017.

[8] Y. Qureshi, M. Tarfaoui, K. K. Lafdi, and K. Lafdi, ñDevelopment of microscale flexible nylon/Ag strain sensor wire for real-time monitoring and damage detection in composite structures subjected to three-point bend test,ò *Compos. Sci. Technol.*, vol. 181, p. 107693, 2019.

[9] J.-B. Ihn and F.-K. Chang, ñPitch-catch active sensing methods in structural health monitoring for aircraft structures,ò *Struct. Heal. Monit.*, vol. 7, no. 1, pp. 5ï 9, 2008.

[10] Y. Qureshi, M. Tarfaoui, K. K. Lafdi, and K. Lafdi, ñReal-time strain monitoring performance of flexible Nylon/Ag conductive fiber,ò *Sensors Actuators A Phys.*, vol. 295, pp. 612ï 622, 2019.

[11] Y. Qureshi, M. Tarfaoui, K. K. Lafdi, and K. Lafdi, ñReal-time strain monitoring and damage detection of composites in different directions of the applied load using a microscale flexible Nylon/Ag strain sensor,ò *Struct. Heal. Monit.*, vol. 0, no. 0, p. 1475921719869986.

[12] Y. Qureshi, M. Tarfaoui, K. K. Lafdi, and K. Lafdi, ñIn-situ Monitoring, Identification and Quantification of Strain Deformation in Composites under Cyclic Flexural Loading using Nylon/Ag Fiber Sensor,ò *IEEE Sens. J.*, p. 1, 2020.

[13] C. Bois, P. Herzog, and C. Hochard, ñMonitoring a delamination in a laminated composite beam using in-situ measurements and parametric identification,ò *J. Sound Vib.*, vol. 299, no. 4, pp. 786ï 805, 2007.

[14] V. Giurgiutiu, A. Zagrai, and J. J. Bao, ñPiezoelectric Wafer Embedded Active Sensors

for Aging Aircraft Structural Health Monitoring,ò *Struct. Heal. Monit.*, vol. 1, no. 1, pp. 41ï 61, 2002.

[15] G. Park, H. H. Cudney, and D. J. Inman, ñAn Integrated Health Monitoring Technique Using Structural Impedance Sensors,ò *J. Intell. Mater. Syst. Struct.*, vol. 11, no. 6, pp. 448ï 455, 2000.

[16] C. C. Ciang, J.-R. Lee, and H.-J. Bang, ñStructural health monitoring for a wind turbine system: a review of damage detection methods,ò *Meas. Sci. Technol.*, vol. 19, no. 12, p. 122001, Oct. 2008.

[17] T. G. Gerardi, ñHealth Monitoring Aircraft,ò *J. Intell. Mater. Syst. Struct.*, vol. 1, no. 3, pp. 375ï 385, 1990.

[18] C. R. Farrar and K. Worden, ñAn introduction to structural health monitoring,ò *Philos. Trans. R. Soc. A Math. Phys. Eng. Sci.*, vol. 365, no. 1851, pp. 303ï 315, 2007.

[19] J. Leng and A. Asundi, ñStructural health monitoring of smart composite materials by using EFPI and FBG sensors,ò *Sensors Actuators A Phys.*, vol. 103, no. 3, pp. 330ï 340, 2003.

[20] W. Staszewski, C. Boller, and G. R. Tomlinson, *Health monitoring of aerospace structures: smart sensor technologies and signal processing*. John Wiley & Sons, 2004.

[21] Y. ZOU, L. TONG, and G. P. STEVEN, ñVIBRATION-BASED MODEL-DEPENDENT DAMAGE (DELAMINATION) IDENTIFICATION AND HEALTH MONITORING FOR COMPOSITE STRUCTURES ð A REVIEW,ò *J. Sound Vib.*, vol. 230, no. 2, pp. 357ï 378, 2000.

[22] A. C. Raghavan and C. Cesnik, ñReview of Guided-Wave Structural Health Monitoring,ò *Shock Vib. Dig.*, vol. 39, pp. 91ï 114, 2007.

[23] S. W. Doebling, C. R. Farrar, M. B. Prime, and D. W. Shevitz, ñDamage identification and health monitoring of structural and mechanical systems from changes in their vibration characteristics: A literature review.ò

[24] J. P. Andrews, A. N. Palazotto, M. P. DeSimio, and S. E. Olson, ñLamb Wave Propagation in Varying Isothermal Environments,ò *Struct. Heal. Monit.*, vol. 7, no. 3, pp. 265ï 270, 2008.

[25] R. Schueler, S. P. Joshi, and K. Schulte, ñDamage detection in CFRP by electrical conductivity mapping,ò *Compos. Sci. Technol.*, vol. 61, no. 6, pp. 921ï 930, 2001.

[26] A. Kunadt, E. Starke, G. Pfeifer, and C. Cherif, ñMesstechnische Eigenschaften von Dehnungssensoren aus Kohlenstoff-Filamentgarn in einem VerbundwerkstoffMeasuring Performance of Carbon Filament Yarn Strain Sensors Embedded in a Composite,ò *tm-Technisches Mess. Plattf. für Methoden, Syst. und Anwendungen der Messtechnik*, vol. 77, no. 2, pp. 113ï 120, 2010.

[27] H. C. H. Li, I. Herszberg, C. E. Davis, A. P. Mouritz, and S. C. Galea, ñHealth monitoring of marine composite structural joints using fibre optic sensors,ò *Compos. Struct.*, vol. 75, no. 1, pp. 321ï 327, 2006.

[28] J. Rausch and E. Mäder, ñHealth monitoring in continuous glass fibre reinforced thermoplastics: Tailored sensitivity and cyclic loading of CNT-based interphase sensors,ò *Compos. Sci. Technol.*, vol. 70, no. 13, pp. 2023ï 2030, 2010.

[29] M. M. B. Hasan, A. Matthes, P. Schneider, and C. Cherif, ñApplication of carbon filament (CF) for structural health monitoring of textile reinforced thermoplastic composites,ò *Mater. Technol.*, vol. 26, no. 3, pp. 128ï 134, 2011.

[30] J. Rausch and E. Mäder, ñHealth monitoring in continuous glass fibre reinforced thermoplastics: Manufacturing and application of interphase sensors based on carbon nanotubes,ò *Compos. Sci. Technol.*, vol. 70, no. 11, pp. 1589ï 1596, 2010.

[31] J. Rausch and E. Mäder, ñCarbon nanotube coated glass fibres for interphase health monitoring in textile composites,ò *Mater. Technol.*, vol. 26, no. 3, pp. 153ï 158, 2011.

[32] N. Forintos and T. Czigany, ñReinforcing carbon fibers as sensors: The effect of temperature and humidity,ò *Compos. Part A Appl. Sci. Manuf.*, vol. 131, p. 105819, 2020.

[33] I. Krucinska and T. Stypka, ñDirect measurement of the axial poissonôs ratio of single carbon fibres,ò *Compos. Sci. Technol.*, vol. 41, no. 1, pp. 1ï 12, 1991.

[34] S. Blazewicz, B. Patalita, and P. Touzain, ñStudy of piezoresistance effect in carbon fibers,ò *Carbon N. Y.*, vol. 35, no. 10, pp. 1613ï 1618, 1997.

[35] C. N. Owston, ñElectrical properties of single carbon fibres,ò *J. Phys. D. Appl. Phys.*, vol. 3, no. 11, pp. 1615ï 1626, Nov. 1970.

[36] A. Horoschenkoff, T. Mueller, and A. Kroell, ñOn the characterization of the piezoresistivity of embedded carbon fibres,ò *ICCM 17th*, 2009.

[37] A. Horoschenkoff, M. Derks, T. Mueller, H. Rapp, and S. Schwarz, ñKonzeptstudie zum einsatz von elektrisch kontaktierten carbonfasern als sensor für leichtbaustrukturen aus

faserverbundwerkstoff Vorträge. 14,ò in *Nationales Symp. Sampe Deutschland eV (Garching, 7--28 February)*, 2008.

[38] P. C. CONOR and C. N. OWSTON, ñElectrical Resistance of Single Carbon Fibres,ò *Nature*, vol. 223, no. 5211, pp. 1146ï 1147, 1969.

[39] J. Wen, Z. Xia, and F. Choy, ñDamage detection of carbon fiber reinforced polymer composites via electrical resistance measurement,ò *Compos. Part B Eng.*, vol. 42, no. 1, pp. 77ï 86, 2011.

[40] C. Luan, X. Yao, H. Shen, and J. Fu, ñSelf-Sensing of Position-Related Loads in Continuous Carbon Fibers-Embedded 3D-Printed Polymer Structures Using Electrical Resistance Measurement,ò *Sensors (Basel).*, vol. 18, no. 4, p. 994, Mar. 2018.

[41] X. Yao, C. Luan, D. Zhang, L. Lan, and J. Fu, ñEvaluation of carbon fiber-embedded 3D printed structures for strengthening and structural-health monitoring,ò *Mater. Des.*, vol. 114, pp. 424ï 432, 2017.

[42] Y. Goldfeld, S. Ben-Aarosh, O. Rabinovitch, T. Quadflieg, and T. Gries, ñIntegrated self-monitoring of carbon based textile reinforced concrete beams under repeated loading in the un-cracked region,ò *Carbon N. Y.*, vol. 98, pp. 238ï 249, 2016.

[43] F.-Y. Yeh, K.-C. Chang, and W.-C. Liao, ñExperimental Investigation of Self-Sensing Carbon Fiber Reinforced Cementitious Composite for Strain Measurement of an RC Portal Frame,ò *Int. J. Distrib. Sens. Networks*, vol. 11, no. 11, p. 531069, 2015.

[44] A. Todoroki, Y. Samejima, Y. Hirano, and R. Matsuzaki, ñPiezoresistivity of unidirectional carbon/epoxy composites for multiaxial loading,ò *Compos. Sci. Technol.*,

vol. 69, no. 11, pp. 1841ï 1846, 2009.

[45] N. Angelidis, C. Y. Wei, and P. E. Irving, ñThe electrical resistance response of continuous carbon fibre composite laminates to mechanical strain,ò *Compos. Part A Appl. Sci. Manuf.*, vol. 35, no. 10, pp. 1135ï 1147, 2004.

[46] J. B. Park, T. Okabe, N. Takeda, and W. A. Curtin, ñElectromechanical modeling of unidirectional CFRP composites under tensile loading condition,ò *Compos. Part A Appl. Sci. Manuf.*, vol. 33, no. 2, pp. 267ï 275, 2002.

[47] H. Khayyam *et al.*, ñPAN precursor fabrication, applications and thermal stabilization process in carbon fiber production: Experimental and mathematical modelling,ò *Prog. Mater. Sci.*, vol. 107, p. 100575, 2020.

[48] J. Sebastian *et al.*, ñHealth monitoring of structural composites with embedded carbon nanotube coated glass fiber sensors,ò *Carbon N. Y.*, vol. 66, pp. 191ï 200, 2014.